Journal of Microscopy and Ultrastructure 3 (2015) 181–190

Contents lists available at ScienceDirect

Journal of Microscopy and Ultrastructure

journal homepage: www.elsevier.com/locate/jmau

Original Article

Histological and immunohistochemical study of the effect of gold nanoparticles on the brain of adult male albino rat

Ezzat Abd El Aziz El-Drieny [a], Naglaa Ibrahim Sarhan [a,*], Naglaa Ahmed Bayomy [a], Said Abd Elmajied Elsherbeni [b], Rania Momtaz [b], Hossam El-Din Mohamed [b]

[a] Histology Department, Faculty of Medicine, Tanta University, Egypt
[b] Medical Applications of Lasers (MAL) Department, National Institute of Laser Enhanced Sciences (NILES), Cairo University, Egypt

ARTICLE INFO

Article history:
Received 6 February 2015
Received in revised form 21 April 2015
Accepted 2 May 2015
Available online 11 May 2015

Keywords:
Gold nanoparticles (GNPs)
GFAP
Brain
Astrogliosis

ABSTRACT

Gold nanoparticles (GNPs) have numerous medical applications as in biological imaging, cancer treatment and in implants (pacemakers and stents). Many conflicting results about GNPs safety and its accumulation in liver, kidney and brain were recorded. This work was carried out to study the histological effect of long period exposure to gold nanoparticle on the brain of adult male albino rat. Twenty adult male albino rats were divided into two equal groups: The first one served as a control group and the second one received 400 μg/kg/day GNPs by gastric tube once daily for eight weeks. Brain specimens were collected at the end of the experiment for histological and immunohistochemical studies using caspase-3 and glial fibrillary acidic protein (GFAP). GNPs treated group revealed wide spread histological alterations and deposition of gold nanoparticle aggregates in the neurons of cerebral cortex and hippocampus and also in the epithelium of choroid plexus with hyalinization of the wall of some blood vessels and disruption of the capillaries. All these changes were associated with localized positive caspase 3 reaction. Various degrees of astrogliosis were evidenced by astrocytic proliferation and increase size of their cell body with increase number and length of their processes. It could be concluded that repeated exposure of adult male albino rats to gold nanoparticles induced its deposition in the brain in association with histological alterations and various degrees of astrogliosis.

1. Introduction

Cancer can be treated by various lines of treatment including surgery, chemo, radio and immunotherapy. Recently nanotechnology holds the promise of treating cancer using lower concentrations of chemotherapeutic agents and target malignant cells while leaving healthy cells untouched [1].

Nanomaterials are characterized by their tiny size which is less than 100 nanometers, approximately 100,000 times smaller than the diameter of a human hair. Nano-sized particles exist in nature and can be created from carbon or minerals like silver and gold. Creating and engineering materials to such a small scale, allow them to acquire on unique therapeutic, electrical and optical properties [2,3]. Gold nanoparticle biomolecule (GNPs) are largely used as bio-markers and biodelivery vehicles in the medicine, pharmacy and in cosmetic products [4,5]. Nano-sized particles can enter the human body through inhalation and ingestion and through the skin [2]. Orally administrated

* Corresponding author. Tel.: +20 1005686375; fax: +20 403407734.
E-mail address: aymkhalil41@hotmail.com (N.I. Sarhan).

http://dx.doi.org/10.1016/j.jmau.2015.05.001
2213-879X/

GNPs appeared in various tissues in mice and the amount of absorption and distribution in the body inversely correlated with the size of the particles [6]. In most studies, systemically administrated NPs were primarily taken up by liver and spleen in a large quantity and small amounts distributed in the lung, kidney, heart, and brain after single administration [6,7].

However, for the therapeutic application and drug delivery of GNPs it is essential to know the distribution and local or systemic toxicity associated with them and whether they have the ability to cross the blood–brain barrier to reach the nervous tissue or not. For this purpose, this study was carried out to assess the potential consequences of oral administration gold nanoparticle on the brain of adult male albino rat.

2. Materials and methods

2.1. Chemicals

2.1.1. Preparation of gold chloride nanoparticles (GNPs)

GNPs (15 nm size) were synthesized according to Levy et al. [8] by citrate reduction of chloroauric acid ($HAuCl_4$). This causes gold(III) auric ($Au3^+$) ions to be reduced to neutral gold atoms. As much of these gold atoms form, the solution becomes supersaturated, and gold gradually precipitated in the form of sub-nanometer particles. The colloidal GNPs solution was filtered through 0.45 μm Millipore syringe filters to get rid of any precipitate; the pH was adjusted to 7 using dilute NaOH solution, and the filtrate was stored at 4 °C [8,9].

During the synthesis of GNPs, a 1 nM solution was prepared. To obtain the desired dose, 10 ml of the 1 nM solution was centrifuged at 13,500 rpm for 10 min and the obtained pellet was re-suspended in sodium citrate 1.2 mM to obtain 10 nM (110 μg of gold/ml). The solution was dark red in color. Gold nanoparticle characterization was carried by spectrophotometer and transmission electron microscopy [9].

Spectrophotometry is used to identify gold nanoparticles in the prepared solutions. The electronic UV-Visible absorption spectrum was recorded on a Perkin Elmer lambda-17 spectrophotometer using a quartz cell with a path length of 1 cm. Spectrophotometry of gold nanoparticles showed strong light absorption in the visible region of the optical spectrum with a maximum of absorbance centered at 520 nm.

Transmission electron microscopy (TEM, Hitachi HU-11B) at 80 kV was used to determine the size and shape of GNPs. The aqueous solution of gold nanoparticle was drop cast onto a carbon coated copper grid, and the grid was air dried at room temperature. The grids loaded with nanoparticles were examined by electron microscope. Quantitative analysis of nanoparticles size was performed by measuring the core diameter of 200 individual particles from multiple micrographs. All these procedures were carried in National Institute of Laser Enhanced Sciences – Cairo University. The prepared gold nanoparticles were spherical in shape and about 15 nm in size.

2.2. Animals

This work was carried out on 20 adult male albino rats weighing 180–200 g. Experimental protocol was approved by the local ethical Committee of Faculty of Medicine, Tanta University, Egypt prior to the study and the animal care was carried out according to the national guidelines for animal care. Drinking water and conventional food were provided ad libitum. Animals were divided into two equal groups. The first one served as a control group and kept without treatment throughout the whole period of the experiment. The second one served as an experimental group and received orally 400 μg/kg/day for 8 weeks of solutions of 110 μg of gold NPs/ml by gastric tube [6]. At the end of the eight weeks, animals were anesthetized and decapitated and the brain was harvested by careful rapid dissection and was immediately fixed in 4% paraformaldehyde for both histological and immunohistochemical study.

2.3. Histological and Immunohistochemical study

For histological study, coronal brain sections were cut and processed for paraffin sections of 5 μm thickness to be stained with Hematoxylin and Eosin [10].

Immunohistochemical detection of caspase-3 and Glial fibrillary acidic protein (GFAP) were performed using primary rabbit anti-rat caspase-3 antibody and primary rabbit anti-GFAP antibody respectively from Neo Markers Fremont CA, Lab Vision. The avidin–biotin complex technique was used. Positive reaction for caspase 3 was visualized as brown coloration of the cytoplasm of the neural cells, while positive reaction for Glial fibrillary acidic protein was visualized as brown coloration of the astrocytes including their bodies and their processes. Negative controls were done using the same steps except that phosphate buffered saline was applied instead of the primary antibodies [11]. All these procedures were carried in the Histology Department of Faculty of Medicine Tanta University.

2.4. Quantitative evaluation of immunolabeled sections

Each immunolabeled section was observed at 400× magnification. The number of caspase 3 positive neurons was recorded in the cerebral cortex, hippocampus and in the choroidal plexus in 10 nonoverlapping fields in slides of each animal of each group. Also, the number of GFAP positive cells was recorded in the cerebral cortex and hippocampus in 10 nonoverlapping fields in slides of each animal of each group. Only process-bearing astrocytes with their nuclei in the plane of the section were considered. Also the number of astrocytic processes, the diameter of astrocytic cell bodies, and the length of the processes were counted and measured. Counting and morphometric analysis were carried out in EM unit of Faculty of medicine Tanta University using image J 1.47 software (Wayne Rasband, USA). All data were analyzed using Student's *t*-test for comparison of the means, taking $P < 0.05$ as significance level [12].

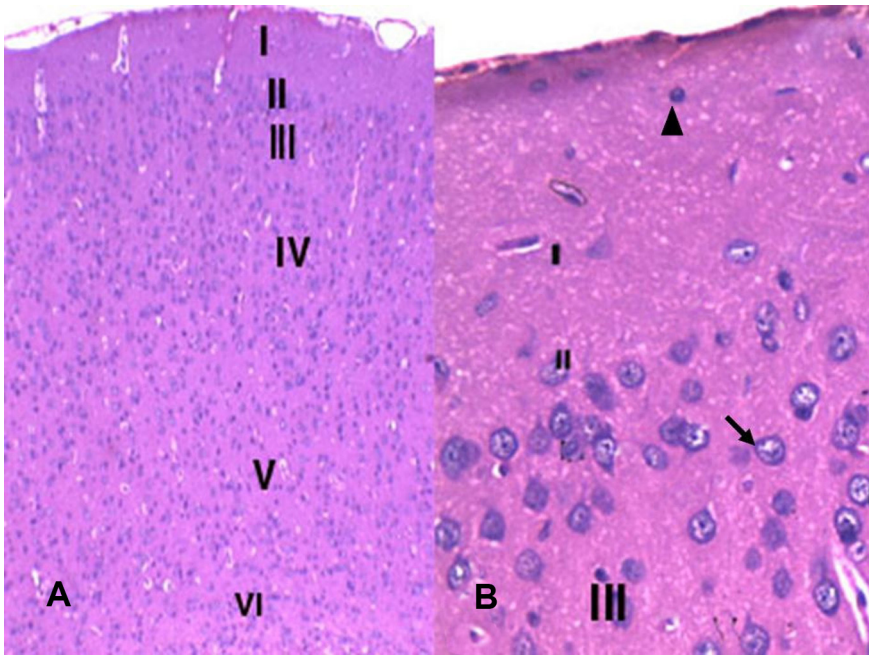

Fig. 1. Showing six layers of cerebral cortex of control group; molecular layer (I), outer granular layer (II), outer pyramidal layer (III), inner granular layer (IV), inner pyramidal layer (V) and polymorphic layer (VI). These layers showing acidophilic neuropile and rounded open face nuclei with prominent nucleoli (→) of the neurons and also of neuroglial cells without properly seen cytoplasm (►). H&E, (A) ×100; (B) H&E, ×400.

3. Results

3.1. Histological results

3.1.1. Hematoxylin and eosin

Light microscopic examination of hematoxylin and eosin stained sections of cerebral cortex of adult male albino rat of control group revealed six distinguished layers with no sharp boundaries in association small blood vessels in between. These layers were; plexiform layer of fibers traveling parallel to the surface with relatively few cells, external granular layer, small pyramidal cell layer, inner granular layer, inner layer of large pyramidal cells and finally the layer of polymorphic cells (Fig. 1). The

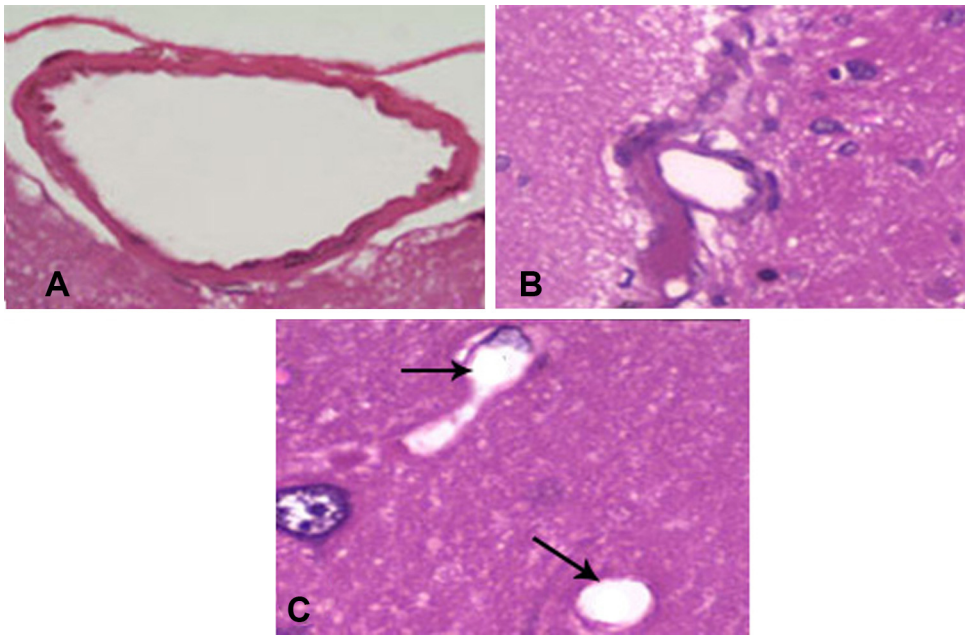

Fig. 2. Brain of control group showing large (A) and medium sized blood vessel (B) and continuous wall of blood capillaries (→) (C). H&E, ×1000.

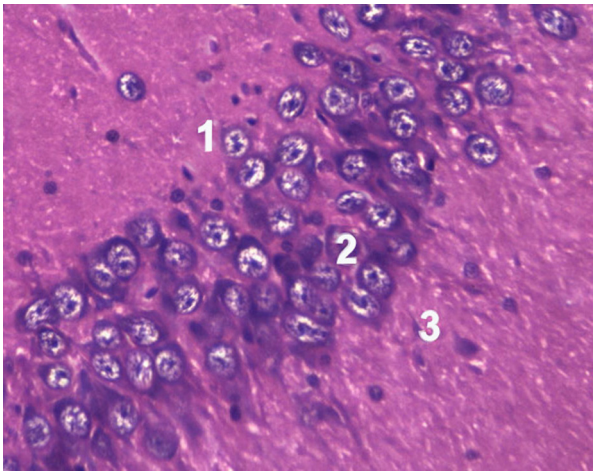

Fig. 3. Hippocampus of control brain with its characteristic three layer: polymorphic layer (1), pyramidal layer (2) and the molecular layer (3). H&E, ×1000.

neuronal cells of all these areas contain oval or rounded open face nuclei with prominent nucleoli surrounded by basophilic cytoplasm. In the neuropile of these layers, many blood vessels of different sizes were seen together with nuclei of neuroglial cells without properly seen cytoplasm (Fig. 2). High power examination of hippocampus revealed three layer; molecular, pyramidal and polymorphic layers (Fig. 3). The choroid plexus consisted of a layer of cuboidal epithelial cells (ependymal cells) surrounding a core of capillaries and loose connective tissue (Fig. 4).

The gold nanoparticle treated group (group II) revealed brown deposits in the neuropile of the cerebral cortex (Fig. 5) and also in the hippocampus (Fig. 6). Also some neuronal cells appeared darkly stained irregular, distorted and shrunken with pericellular haloes together with darkly stained nuclei (Figs. 5 and 6). Brain of GNPs treated group showed large sized and medium sized BV with hyalinization and GNPs deposition in their wall. The blood capillaries revealed disruption of their wall (Fig. 7). The cytoplasm

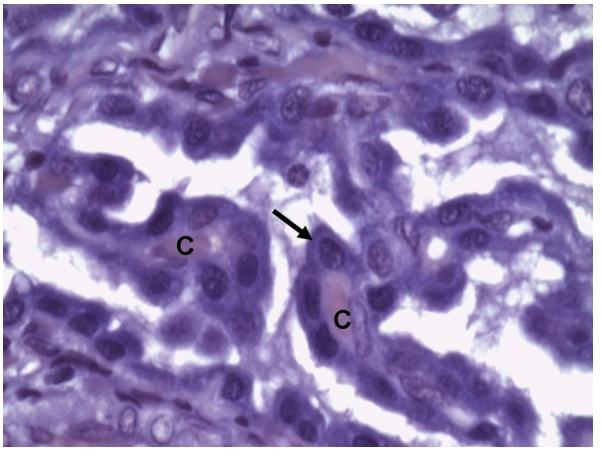

Fig. 4. Choroid plexus of brain of control group showing ependymal cells (→) surrounding blood capillaries (C). H&E, ×1000.

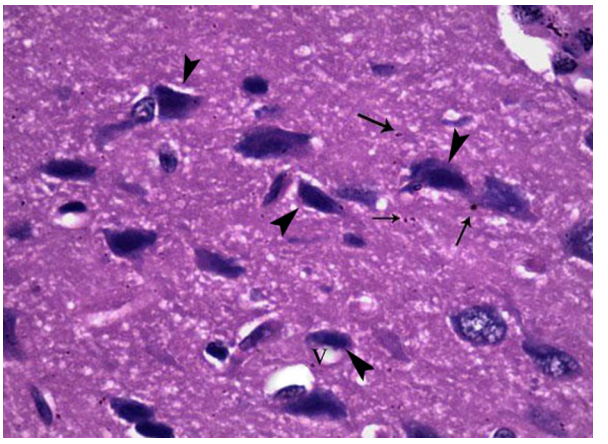

Fig. 5. Cerebral cortex of gold nanoparticle treated group showing aggregates of gold nanoparticles in the neuropile of the cerebral cortex (→) together with distorted darkly stained neurons with darkly stained nuclei (►) and intracytoplasmic vacuoles (V). H&E, ×1000.

of some ependymal cells of the choroids displayed brown deposits (Fig. 8).

3.1.2. *Immunohistochemical study*

The control group (group I) revealed negative immunostaining reaction for caspase-3 in all areas of the cerebral

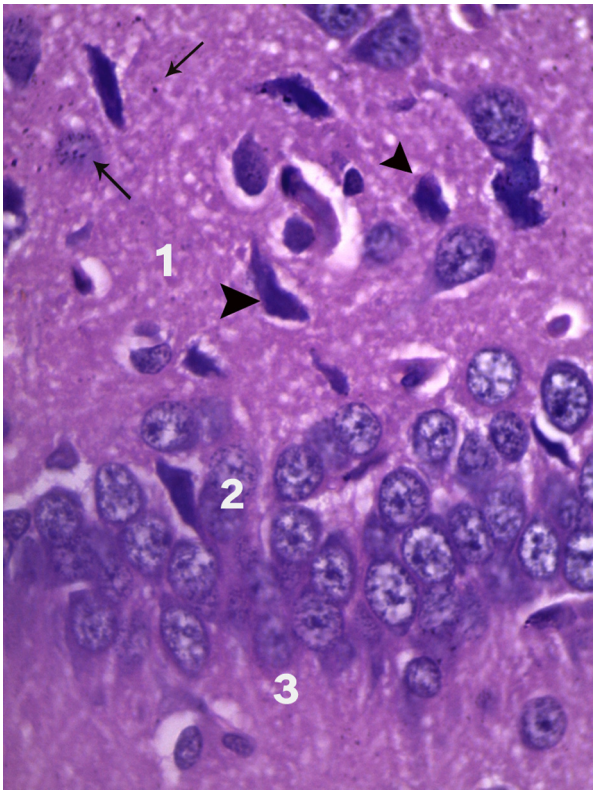

Fig. 6. Hippocampus with its characteristic three layers) polymorphic 1, pyramidal 2 and molecular 3 (of gold nanoparticle treated group showing aggregates of gold nanoparticles in the neuropile (→). Some neuronal cells appeared darkly stained shrunken with per cellular' haloes (►). H&E, ×1000.

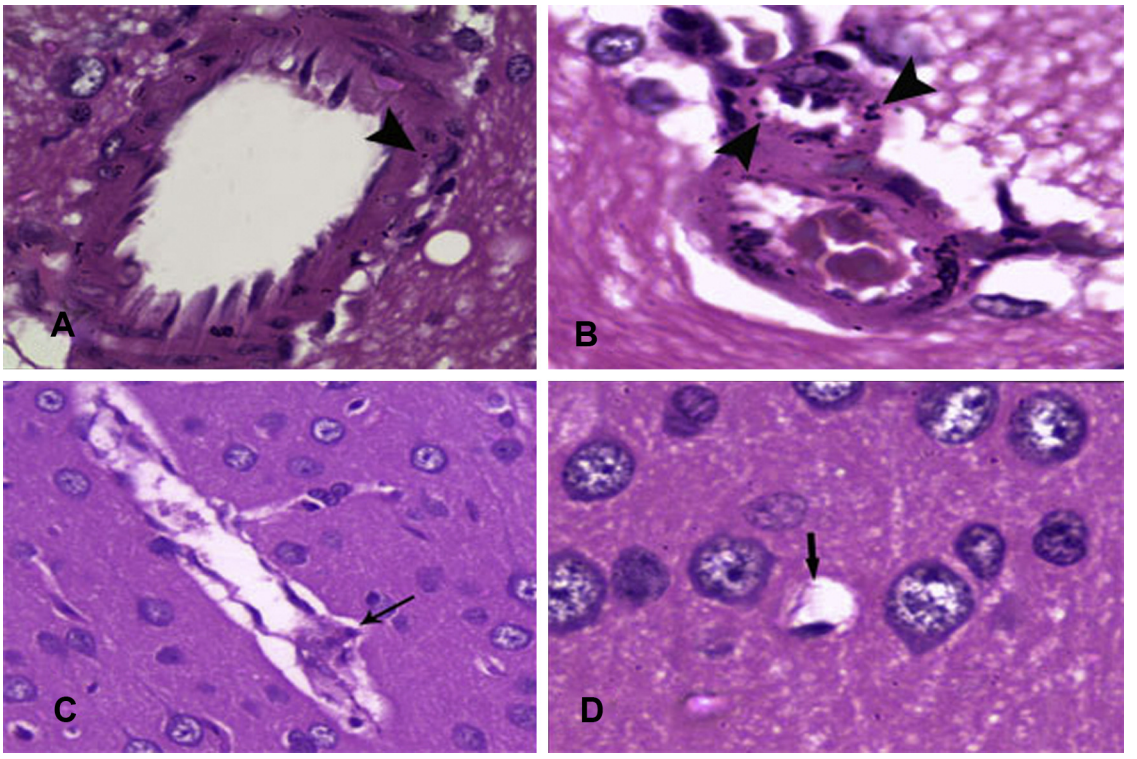

Fig. 7. Brain of GNPs treated group showing large sized BV (A) and medium sized BV (B) with hyalinization of their walls and GNPs deposition. Notice disruption of the wall of blood capillaries (C&D) (→). H&E, ×1000.

cortex (Fig. 9A) and also in the hippocampus (Fig. 9B). The choroid showed few localized mildly positive choroidal epithelial cells for active caspase 3 (Fig. 10). Similarly, gold nanoparticle treated animals revealed negative caspase 3 reaction in the cerebral cortex and only few positive neurons were seen in the hippocampus (Fig. 11). On the other hand, choroidal epithelium of the same group showed strong positive reaction for active caspase-3 in many cells (Fig. 12).

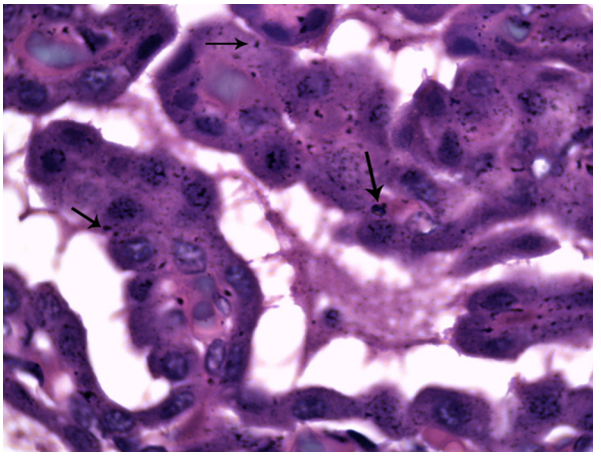

Fig. 8. Choroidal plexus of gold nanoparticle treated group showing brown deposits of GNPs in the cytoplasm of ependymal cells (→). H&E, ×1000.

Cerebral cortex and hippocampus of the control group showed widely apart small sized GFAP positives astrocytes with few short process (Fig. 13). The GNPs treated group showed different degrees of astrogliosis. This was in the form of astrocytic proliferation and increase size of their cell body with increase number and length of their processes. Some areas of cerebral cortex displayed moderate astrogliosis manifested by preservation of individual astrocyte and without pronounced overlap of astrocyte processes (Fig. 14A). Other areas displayed diffuse reactive astrogliosis evidenced by pronounced overlap of astrocyte processes with strong expression for GFAP (Fig. 15A). Also the hippocampus revealed strong immunoreaction and hypertrophy of astrocytes with different degree of astrogliosis (Figs. 14B and 15B).

3.2. Morphometric and statistical analysis

No significant difference in the number of caspase 3 positive neurons in the GNPS treated group compared with control group as regard cerebral cortex and hippocampus. However, there was significant increase in the caspase 3 positive immunoreaction of the choroidal epithelium cells in the GNPS treated group (Table 1). Morphometric analysis revealed that the number of immunoreactive astrocytes in the control group was more numerous in hippocampus more than cerebral cortex. Significant increase in the GFAP-immunoreactive astrocytes was also observed in the brain of gold nano particles treated group in comparison to control group with specific predominance in the hippocampus

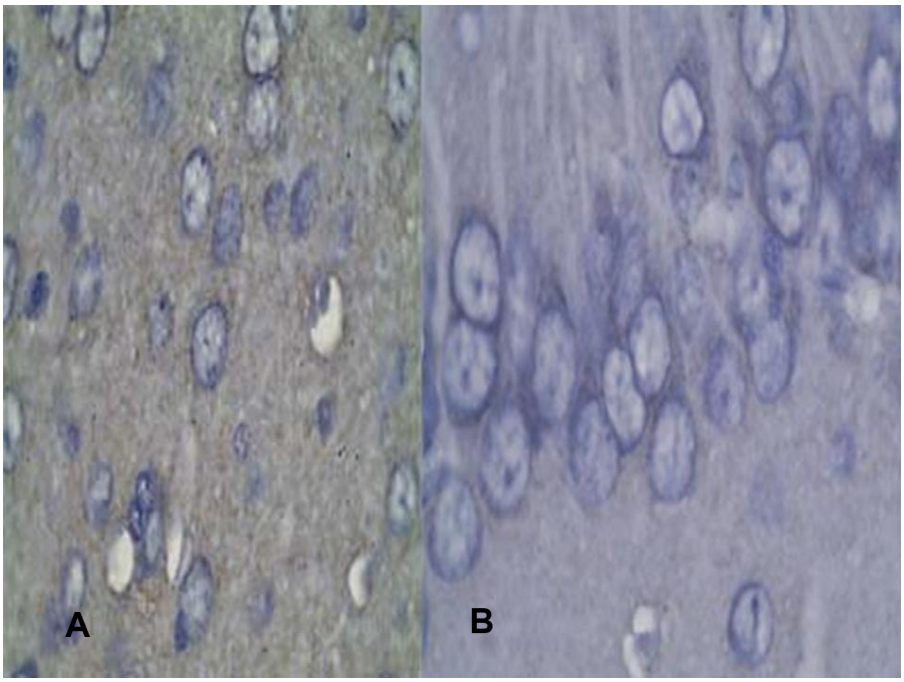

Fig. 9. Cerebral cortex (A) and hippocampus (B) of brain of control group showing negative immune reaction for caspase-3. Caspase 3 immunostaining, ×1000.

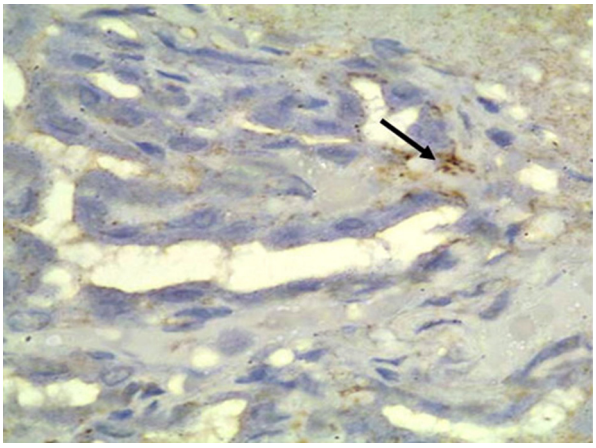

Fig. 10. Choroid plexus of control group showing few mildly positive cells for active caspase-3 in the choroid epithelial cell. Caspase 3 immunostaining, ×1000.

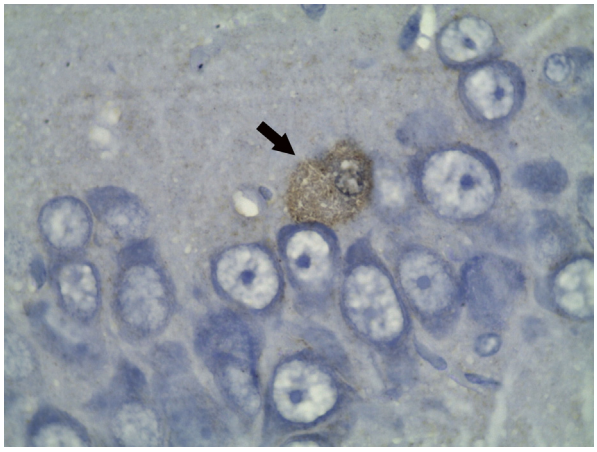

Fig. 11. Hippocampus of GNPs treated group showing positive neuron for active caspase 3 (→). Caspase 3 immunostaining, ×1000.

Table 1
Mean value of number of caspase-3 positive cells and GFAP positive astrocytes in cerebral cortex and hippocampus of the studied groups.

Measured parameters	Control	GNPs group	"*t*" value	*P* value
Number of caspase-3 positive neurons in cerebral cortex	0.75 ± 0.45	0.833 ± 0.577	0.394	0.698
Number of caspase-3 positive neurons in hippocampus	1.26 ± 0.703	1.46 ± 0.516	0.887	0.382
Number of caspase-3 positive cells in choroidal epithelium	1.86 ± 0.351	5.133 ± 1.407	8.72	0.000
Number of GFAP positive astrocytes in cerebral cortex	7.083 ± 1.76	12.028 ± 3.24	6.79	0.003
Number of GFAP positive astrocytes in hippocampus	11.75 ± 2.251	17.25 ± 2.712	4.413	0.001

Data expressed as mean ± standard deviation, *t* = Student (*t*) test, *P* value = probability of chance, $P < 0.05$ is significant.

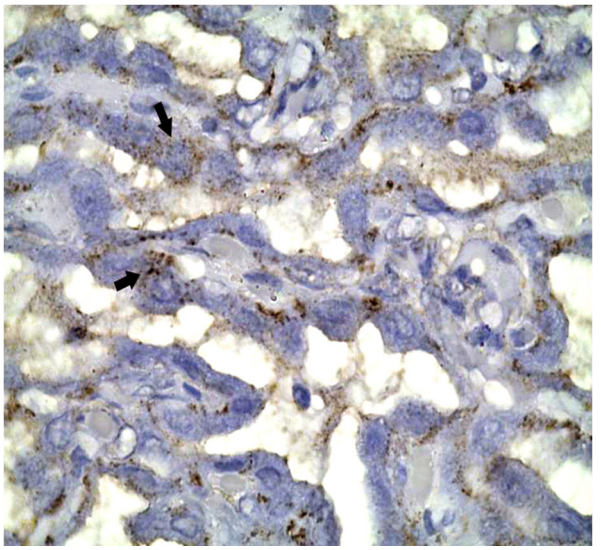

Fig. 12. Choroid plexus of GNPs treated group showing many positive choroidal epithelial cells for active caspase 3 (→). Caspase 3 immunostaining, ×1000.

compared to cerebral cortex (Table 1). Similarly the diameters of astrocyte cell bodies, the length and the numbers of their processes were significantly increased in the brain of GNPs treated group compared to control one (Table 2).

4. Discussion

The present study demonstrated that gold nanoparticles administration displayed histological alterations in the neurons of the cerebral cortex and in the hippocampus in association with brown deposits in their cells and neuropile and in the choroidal epithelium. All these changes were associated with positive caspase 3 reaction in few neurons and in the choroidal epithelium with different degrees of astrogliosis.

The presence of GNPs in the brain tissue was similar to several previously reported publications like Hyllier and Albertch [13] who observed GNPs (from 4 to 58 nm) in various tissues of mice including brain after single oral administration. Others investigators [14] performed a kinetic study to evaluate the GNPs size (10, 50, 100 and 250 nm) effects on the in vivo tissue distribution of nanoparticles in the rat 24 h after injection. The authors showed that the tissue distribution of GNPs is size dependent with the smallest 10 nm gold nanoparticles possessing the most widespread organ distribution, whereas no GNP was detected for larger 50 nm. Reports have shown that GNPs appear in various tissues after one and seven days of intravenous administration [15]. Similar results have been obtained with repeated intraperitoneal administration of 12.5 nm GNPs in mice once daily for eight weeks [6].

The presence of gold nanoparticles in the brain of GNPs treated group and in the wall of the blood vessels as presented in this study were attributed to two different mechanisms, firstly by transsynaptic transport after inhalation through the olfactory epithelium, and secondly by its uptake through the blood–brain barrier after its translocation from the lung into the blood resulting in systemic exposure of brain [16,17]. Some studies indicated that the healthy BBB contains defense mechanisms protecting it from blood borne nanoparticle exposure. When nanoparticles with different surface characteristics were assessed,

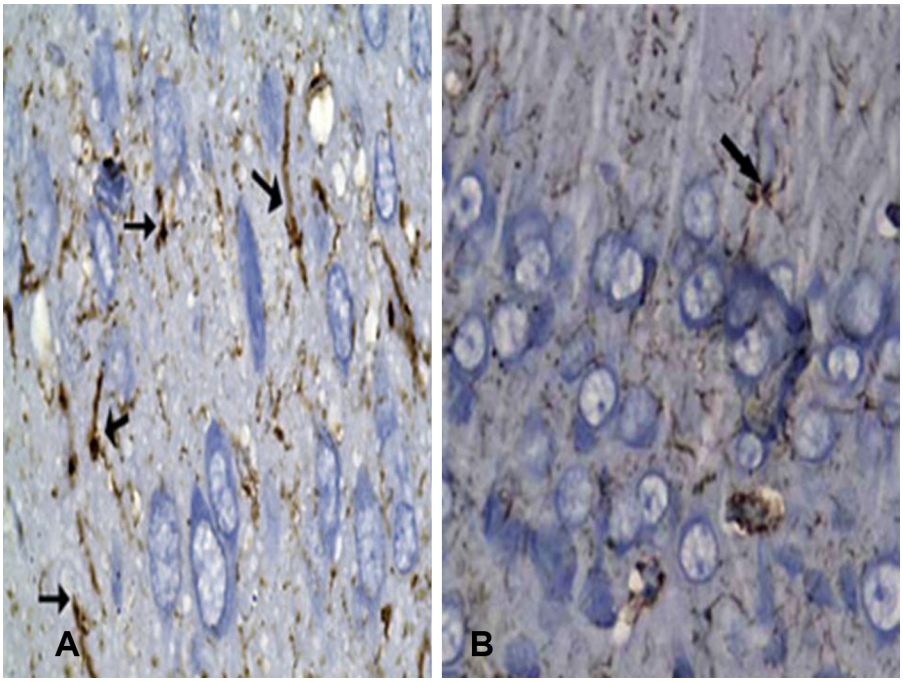

Fig. 13. Cerebral cortex (A) hippocampus (B) of control group showing few widely apart small sized GFAP positive astrocytes with few short processes (→). GFAP immunostaining, ×1000.

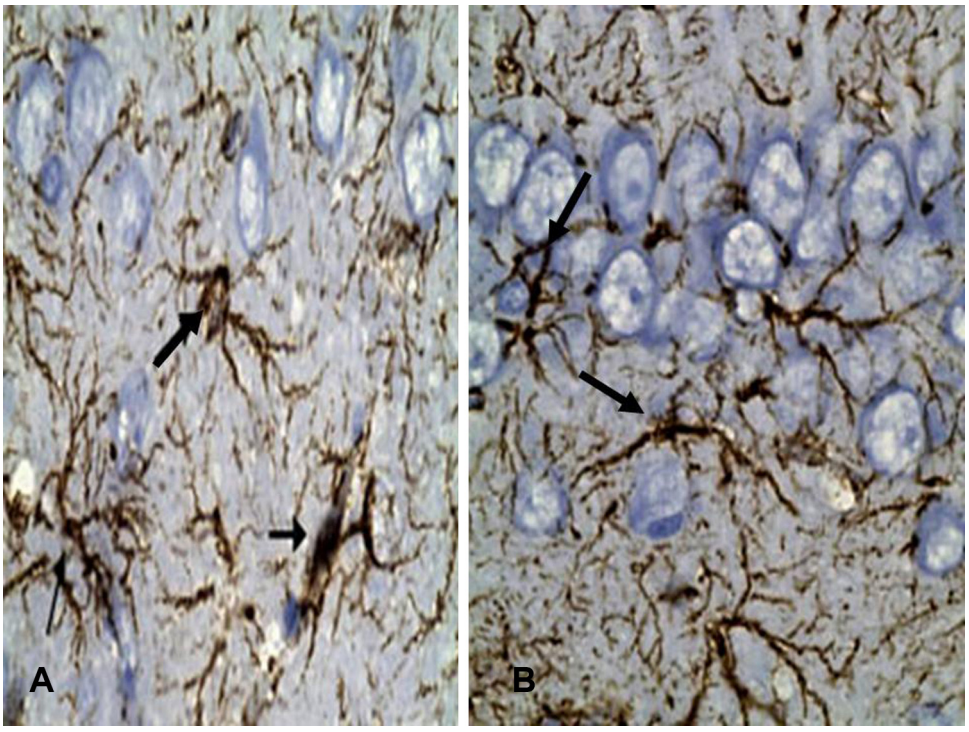

Fig. 14. Cerebral cortex (A) and hippocampus (B) of GNPs treated group showing strongly positive GFAP hypertrophic astrocytes with multiple elongated processes (→) (moderate astrogliosis). GFAP immunostaining, ×1000.

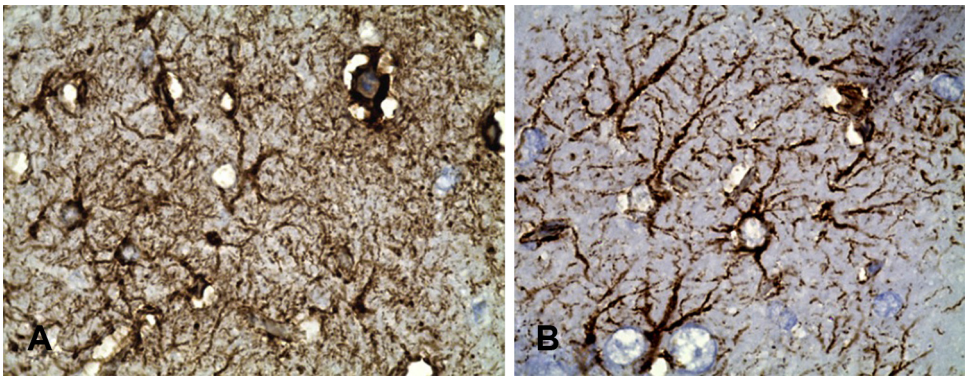

Fig. 15. Cerebral cortex (A) and hippocampus (B) of GNPs treated group showing strong GFAP reaction and hypertrophic astrocytes (severe astrogliosis). GFAP immunostaining, ×1000.

neutral nanoparticles and low concentrations of anionic nanoparticles were detected to have no result on BBB integrity, while on the contrary high concentrations of anionic nanoparticles and cationic nanoparticles were toxic to the BBB [18]. Alzheimer's like pathology was recorded in the brain and it was attributed to increased markers of inflammation and accumulation of 42-amino acid form of beta-amyloid (Abeta42) in frontal cortex and hippocampus in association with the presence of nanoparticles [19].

Previous studies demonstrated that intravenously administered gold nanoparticles to mice could pass through the blood retinal barrier and are distributed in

Table 2
Mean values of diameter of the astrocytes cell bodies and length and number of their processes in the brain of control and gold nanoparticle treated groups.

Measured parameters	Control	GNPs group	"*t*" value	*P* value
Diameter of cell body in μm Mean ± SD	14.63 ± 3.18	20.74 ± 4.12	2.370	0.033
Length of foot processes in μmMean ± SD	17.52 ± 4.98	32.37 ± 7.32	5.519	0.001
Number of foot processes Mean ± SD	3.27 ± 0.64	4.9 ± 0.83	5.153	0.001

Data expressed as mean ± standard deviation, *t* = Student (*t*) test, *P* value = probability of chance, $P < 0.05$ is significant.

all retinal layers without cytotoxicity. It was also found that 20 nm membrane bound nanoparticles in the retinal neurons, endothelial cells and peri-endothelial glial cells [20]. In the retina, cells containing nanoparticles did not show any structural abnormality and increase of cell death compared to cells without nanoparticles. Histologic visualization of GNPs within the brain parenchyma was reported previously suggesting BBB transgression [21]. Nanoparticle-associated toxicity degrade the BBB which may be a factor contributing to nanoparticle access to the brain parenchyma [4].

The morphological changes observed in present work were parallel to the previously reported data of previous researchers who observed moderate hyperemia, pericellular edema, and weak neuronal degeneration in the brain tissue of rats. But the same study did not observe any pathological changes in the brain tissue of rabbits [22]. In consistence with these findings, Fernanda et al. [23] followed the biodistribution of GNPs in mice up to 7 days after intravenous injection of the nanoparticles with near infrared time-domain imaging. They detected the peak concentration in the head of mice was between 19 and 24 h. The precise particle distribution in the brain was mainly accumulated in the hippocampus, thalamus, hypothalamus, and the cerebral cortex [23]. This was contradictory to the work of some investigators [18] who mentioned that both 50 and 15 nm NPs expressed histological changes in the inner organs except for brain where the structural changes were not significant and not size dependent. Similarly, other studies could not demonstrate cytotoxicity in the retina of mice [20] or brain of rat [6] after exposure to GNP. The reason for this difference between our study and the results of others were not apparent, but could be related to the size, shape, surface chemistry, synthesis methods, surface composition of the nanoparticle, duration of exposure and higher concentrations of gold nanoparticle used [24].

Several possible mechanisms for the toxicity of particles in general have been postulated including injury of epithelial tissue [25], inflammation, oxidative stress response [26,27], and allergy [28]. At the cellular level oxidative stress is considered to be of importance [29]. Inflammatory biomarkers such as Interleukin 1α (IL1α) and Tumor Necrosis Factor α (TNFα) were increased in the brain of mice exposed to ambient air particulate matter compared to controls [30,31]. Nanoparticles have been shown to produce reactive oxygen species and oxidative stress [26]. Brain is particularly susceptible to oxidative stress because of its high oxygen consumption rate, it is rich in unsaturated lipids, and it has a relatively high abundance of redox-capable transition metal ions and a relatively low availability of antioxidant enzymes compared with other organs [32]. In a previous study it was concluded that GNPs cause generation of oxidative stress and an impairment of the antioxidant enzyme glutathione peroxidase in rat brain. GNPs also cause generation of 8-hydroxydeoxyguanosine (8OHdG), caspase-3 and heat shock protein 70 (Hsp70), and IFN-γ, which may lead to inflammation and DNA damage/cell death [31].

Astrogliosis was one of the prominent observed finding in the present study. Damaged neurons have long been reported to induce astrogliosis. Astrogliosis has been used as an index for underlying neuronal damage. The mechanism of triggering astrogliosis was attributed to many different types of intercellular signaling molecules including cytokines such as IL6, TNFα, INFγ, TGFβ, FGF2, etc., reactive oxygen species (ROS) including nitric oxide (NO), mediators of innate immunity such as lipopolysaccharide (LPS), neurotransmitters such as glutamate and noradrenaline, purines such as ATP, hypoxia and glucose deprivation, products associated with neurodegeneration such as β-amyloid and regulators of cell proliferation such endothelin-1. Such molecular mediators of reactive astrogliosis can be released by all cell types in CNS tissue, including neurons, oligodendrocyte lineage cells, microglia, endothelia, pericytes, and other astrocytes [33–35]. The potential for 4 nm coated gold nanoparticles was investigated to act as selective carriers across human brain endothelium and subsequently to enter astrocytes. Movement of these nanoparticles occurred across the apical and basal plasma membranes via the cytosol with relatively little vesicular or paracellular migration; antibiotics that interfere with vesicular transport did not block migration. The transfer rate was also based on the surface coating of the nanoparticle and incubation temperature. Using a novel 3-dimensional co-culture system, which includes primary human astrocytes and a brain endothelial cell line hCMEC/D3, it has been demonstrated that the glucose-coated nanoparticles traverse the endothelium, move through the extracellular matrix and localize in astrocytes [36].

5. Conclusions

It could be concluded that repeated exposure of adult male albino rats to gold nanoparticles induced its deposition in various areas of the brain in association with histological alterations and various degrees of astrogliosis.

Conflict of interest

None declared.

Acknowledgements

This work was supported by Faculty of Medicine Tanta university and National Institute of Laser Enhanced Sciences (NILES), Cairo University.

References

[1] Chow EK, Ho D. Cancer nanomedicine from drug delivery to imaging. Sci Transl Med 2013;5(216):216rv4.
[2] Buzea C, Pacheco II, Robbie K. Nanomaterials and nanoparticles: sources and toxicity. Biointerphases 2007;2(4):MR17–71.
[3] Alagarasi A. Introduction to nonmaterials; 2011 http://www.nccr.iitm.ac.in/
[4] Wiley DT, Webster P, Gale A, Davis M. Transcytosis and brain uptake of transferrin-containing nanoparticles by tuning avidity to transferrin receptor. Proc Natl Acad Sci U S A 2013;110(21):8662–7.
[5] Kipp JE. The role of solid nanoparticle technology in the parental delivery of poorly water-soluble drugs. Int J Pharm 2004;284:109–22.
[6] Lasagna-Reeves C, Gonzalez-Romero D, Barria MA, Olmedo I, Clos A, Sadagopa Ramanujam VM, et al. Bioaccumulation and toxicity of

gold nanoparticles after repeated administration in mice. Biochem Biophys Res Commun 2010;393(4):649–55.
[7] Prades R, Guerrero S, Araya E, Molina C, Salas E, Zurita E, et al. Delivery of gold nanoparticles to the brain by conjugation with a peptide that recognizes the transferrin receptor. Biomaterials 2012;33(29):7194–205.
[8] Levy R, Thanh NT, Doty RC, Hussain I, Nichols RJ, Schiffrin DJ, et al. Rational and combinatorial design of peptide capping ligands for gold nanoparticles. J Am Chem Soc 2004;126(32):10076–84.
[9] Kogan MJ, Bastus NG, Amigo R, Grillo-Bosch D, Araya E, Turiel A, et al. Nanoparticle-mediated local and remote manipulation of protein aggregation. Nano Lett 2006;6(1):110–5.
[10] Marilyn G. In: Bancroft JD, Gample M, editors. The hematoxylin and eosin in theory and practice of histological technique. 6th ed. China: Elsevier; 2008. p. 121.
[11] Jackson P, Blythe D. In: Bancroft JD, Gample M, editors. Immunohistochemical techniques in theory and practice of histological technique. 6th ed. China: Elsevier; 2008. p. 423.
[12] Vanzani MC, Iacono RF, Caccuri RL, Berria MI. Immunochemical and morphometric features of astrocyte reactivity vs. plaque location in Alzheimer's disease. Medicina (B Aires) 2005;65(3):213–8.
[13] Hillyer F, Albrecht RM. Gastrointestinal persorption and tissue distribution of differently sized colloidal gold nanoparticles. J Pharm Sci 2001;90:1927–36.
[14] De Jong WH, Hagens WI, Krystek P, Burger MC, Sips AJAM, Geertsma RE. Particle size-dependent organ distribution of gold nanoparticles after intravenous administration. Biomaterials 2008;29:1912–9.
[15] Cho WS, Cho M, Jeong J, Choi M, Cho HY, Han BS, et al. Acute toxicity and pharmacokinetics of 13 nm-sized PEG-coated gold nanoparticles. Toxicol Appl Pharmacol 2009;236:16–24.
[16] Oberdörster G, Oberdörster E, Oberdörster J. Nanotoxicology: an emerging discipline evolving from studies of ultrafine particles. Environ Health Perspect 2005;113(7):823–39.
[17] Yu LE, Yung LYK, Ong CN, Tan YL, Balasubramaniam KS, Hartono D, et al. Translocation and effects of gold nanoparticles after inhalation exposure in rats. Nanotoxicology 2007;1(3):235–42.
[18] Tiwari SB, Amiji MM. A review of nanocarrier-based CNS delivery systems. Curr Drug Deliv 2006;3:219–32.
[19] Calderon-Garciduenas L, Reed W, Maronpot RR, Henríquez-Roldán C, Delgado-Chavez R, Calderón-Garcidueñas A, et al. Brain inflammation and Alzheimer's-like pathology in individuals exposed to severe air pollution. Toxicol Pathol 2004;32(6):650–8.
[20] Kim JH, Kim JH, Kim KW, Kim MH, Yu YS. Intravenously administered gold nanoparticles pass through the blood–retinal barrier depending on the particle size, and induce no retinal toxicity. Nanotechnology 2009;20(50):505101.
[21] Etame AB, Diaz RJ, O'Reilly MA, Smith CA, Mainprize TG, Hynynen K, et al. Enhanced delivery of gold nanoparticles with therapeutic potential into the brain using MRI-guided focused ultrasound. Nanomedicine 2012;8(7):1133–42.
[22] Terentyuk GS, Maslyakova GN, Suleymanova LV, Khlebtsov BN, Kogan BY, Akchurin GG, et al. Circulation and distribution of gold nanoparticles and induced alterations of tissue morphology at intravenous particle delivery. J Biophoton 2009;2(5):292–302.
[23] Sousa F, Mandal S, Garrovo C, Astolfo A, Bonifacio A, Lataw-iec D, et al. Functionalized gold nanoparticles: a detailed in vivo multimodal microscopic brain distribution study. Nanoscale 2010;2(12):2826–34.
[24] Schrand AM, Rahman MF, Hussain SM, Schlager JJ, Smith DA, Syed AF. Metal-based nanoparticles and their toxicity assessment. Wiley Interdiscip Rev Nanomed Nanobiotechnol 2010;2(5):544–68.
[25] Pagan I, Costa DL, McGee JK, Richards JH, Dye JA. Metals mimic airway epithelial injury induced by in vitro exposure to Utah Valley ambient particulate matter extracts. J Toxicol Environ Health A 2003;66:1087–112.
[26] Nel A, Xia T, Madler L, Li N. Toxic potential of materials at the nanolevel. Science 2006;311:622–7.
[27] Donaldson K, Stone V. Current hypotheses on the mechanism of toxicity of ultrafine particles. Ann Ist Super Sanita 2003;39:405–10.
[28] Dybing E, Lovdal T, Hetland RB, Lovik M, Schwarze PE. Respiratory allergy adjuvant and inflammatory effects of urban ambient particles. Toxicology 2004;198:307–14.
[29] Oberdörster G, Oberdörster E, Oberdörster J. Nanotoxicology: an emerging discipline evolving from studies of ultrafine particles. Environ Health Perspect 2005;113:823–39.
[30] Campbell A, Oldham M, Beceria A, Bondy SC, Meacher D, Sioutas C, et al. Particulate matter in polluted air may increase biomarkers of inflammation in mouse brain. Neurotoxicology 2005;26:133–40.
[31] Siddiqi NJ, Abdelhalim MA, El-Ansary AK, Alhomida AS, Ong WY. Identification of potential biomarkers of gold nanoparticle toxicity in rat brains. J Neuroinflammation 2012;9:123.
[32] Uttara B, Singh AV, Zamboni P, Mahajan RT. Oxidative stress and neurodegenerative diseases: a review of upstream and downstream antioxidant therapeutic options. Curr Neuropharmacol 2009;7(1):65–74.
[33] Sofroniew MV. Molecular dissection of reactive astrogliosis and glial scar formation. Trends Neurosci 2009;32:638–47.
[34] Zhang D, Hu X, Qian L, O'Callaghan JP, Hong JS. Astrogliosis in CNS pathologies: is there a role for microglia? Mol Neurobiol 2010;41(2–3):232–41.
[35] Sofroniew MV, Vinters HV. Astrocytes: biology and pathology. Acta Neuropathol (Berl) 2010;119(1):7–35.
[36] Gromnicova R, Davies HA, Sreekanthreddy P, Romero IA, Lund T, Roitt IM, et al. Glucose-coated gold nanoparticles transfer across human brain endothelium and enter astrocytes in vitro. PLOS ONE 2013;8(12):e81043.